

NPS ARCHIVE
1963
MCAFEE, R.

McAfee

CURRENT FLOW IN A THIN FILM
CADMIUM SULFIDE DIODE.

Thesis
M12

CURRENT FLOW IN A THIN FILM CADMIUM
SULFIDE DIODE

by

ROBERT EARL MCAFEE
B.S., U. S. Naval Academy
(1960)

SUBMITTED IN PARTIAL FULFILLMENT OF THE
REQUIREMENTS FOR THE DEGREE OF

MASTER OF SCIENCE

at the

MASSACHUSETTS INSTITUTE OF TECHNOLOGY
June, 1963

Signature of Author _____
Department of Electrical Engineering, May 17, 1963

Certified by _____ Thesis Supervisor

Accepted by _____
Chairman, Departmental Committee on Graduate Students

CURRENT FLOW IN A THIN FILM CADMIUM SULFIDE DIODE

by

ROBERT EARL MCAFEE

Submitted to the Department of Electrical Engineering on May 17, 1963, in partial fulfillment of the requirements for the degree of Master of Science.

ABSTRACT

Diodes were prepared using thin films of cadmium sulfide sandwiched between thin-films, metal electrodes. The current versus voltage characteristics were studied as a function of the manufacturing process and temperature. The variables in the manufacturing process were choice of metals for electrodes, interchange of top and bottom electrode, deposition of an oxide barrier between electrode and insulator, heat treatment of the cadmium sulfide, and variation of the substrate temperature during deposition. From the results obtained, space-charge-limited currents could not be the physical mechanism involved. Instead an argument could be made for a field emission phenomenon at low temperatures with Schottky emission occurring at higher temperatures. The two regions were separated by a sharp transition at a critical temperature.

Thesis Supervisor: James G. Gottling
Title: Assistant Professor of Electrical Engineering

ACKNOWLEDGEMENT

The author would like to express his thanks to Professor J. G. Gottling of the Department of Electrical Engineering for not only the idea behind this thesis, but also for many helpful suggestions along the way. The author is also indebted to Professor M. S. Osmon, J. D. Heightley, and P. Thiesen for constructive criticism and help in some of the experimental techniques. Last, but not least, the author is indebted to his wife who listened patiently to all the failures, cheered for all the successes, and finally typed the finished copy.

TABLE OF CONTENTS

Title Page	1
Abstract	2
Acknowledgement	3
Table of Contents	4
List of Illustrations	5
I. Introduction	6
II. Experimental	8
III. Discussion	13
IV. Conclusion	19
Appendix	20
References	30

LIST OF ILLUSTRATIONS

1. Physical design of diode	8a
2. V-i characteristics of 2145	8a
3. Static V-i characteristics of 2145	8b
4. Variation of characteristics with oxide thickness	10c
5. Log I vs $1/T$ for 2154	10a
6. Log $(1-I_0/T^2)$ vs $1/T$ for 2154	11a
7. Log I vs $V^{1/2}$ for 2154	11a
8. Band model	21a
9. Lindmayer, Reynolds, and Wrigley curve	21a
10. Limiting values of Log J vs Log V	29a

I. INTRODUCTION

Thin film diodes composed of a metal electrode-cadmium sulfide-metal electrode sandwich were evaporated on to a glass substrate with the purpose of obtaining a solid-state analog to a vacuum diode. The theory of space-charge-limited currents in insulators¹⁻⁵ plus the experimentally observed space-charge-limited currents in single crystal of cadmium sulfide⁶ seemed to indicate that such a thin-film device might be feasible. Rectification properties of similar diodes have been observed previously,^{7,8} but little is known about the physical processes involved.

Dresner and Shallcross⁸ attempted to describe the phenomenon as a space-charge-limited current, but were not successful. They found a large discrepancy between the density of traps as indicated by theory and as measured by the method of thermally stimulated currents. The measured density of $10^{21}/\text{cm}^3$ seems more reasonable than the calculated density of $10^{13}/\text{cm}^3$ assuming the i-v relationship was space-charge-limited. Single crystals of cadmium sulfide have been observed to have a trap density of $10^{14}/\text{cm}^3$.

A second point of major difference was the measured capacitance. Lampert has shown that the maximum deviation from the geometrical capacitance is a multiplicative factor

1. Superscripts refer to references at the end of this paper.

From the above discussion of the various experimental

results it is evident that the experimental results are in

agreement with the theory of the origin of the

results to a large extent. The theory of the origin of the

results in the above is in good agreement with the

experimental results. It is evident that the

results are in good agreement with the

theory. The results are in good agreement with the

theory. The results are in good agreement with the

theory. The results are in good agreement with the

theory. The results are in good agreement with the

theory. The results are in good agreement with the

theory. The results are in good agreement with the

theory. The results are in good agreement with the

theory. The results are in good agreement with the

theory. The results are in good agreement with the

theory. The results are in good agreement with the

theory. The results are in good agreement with the

The second point of comparison with the

results. It is evident that the results are in

agreement with the theory. The results are in

The above results are in good agreement with the

of two for space-charge-limited currents. Dresner and Shallcross were unable to observe a capacitance of less than four times the geometric capacitance.

We conclude that space-charge-limited current alone cannot be the basis for this device. This project had as its main purpose the determination of some kind of model for the current flow process. No conclusive answer was reached, but a conjecture as to the correct model was made. First, Schottky emission is dominant at temperatures elevated above a critical temperature and second, below this critical temperature, the dominant process is field emission or tunneling. The critical temperature was observed only experimentally and could not be explained by the theory.

II. EXPERIMENTAL

The diodes were prepared by the evaporation of electrodes and the cadmium sulfide on glass microscope slides. The geometry employed in all samples is shown in figure 1. The method of preparing the slides for deposition has been described by Ceman.¹⁰ During the deposition process, the pressure in the vacuum system was held in the neighborhood of 10^{-5} torr.

The cadmium sulfide used was laboratory grade powder manufactured by B & A Company. This powder was evaporated from open molybdenum boats. At first the substrates were cooled with liquid nitrogen in order to speed the rate of condensation of CdS. It was later found, however, that the resistivity of the films was greatly increased by heating the substrates to 150°C . Several workers have reported using higher substrate temperatures,⁸ and one paper¹¹ reports obtaining resistivities of thin-film cadmium sulfide approaching that of the single crystalline material.

It was found in the earlier work that some of the samples prepared on the cold substrates were ohmic immediately after manufacture. These could be made non-linear by heating in an oven at temperatures of $100\text{--}200^{\circ}\text{C}$ for periods of several hours. This process is similar to that described by Dresner and Shallcross.⁸

Slide 2145 had aluminum as the bottom (common) electrode

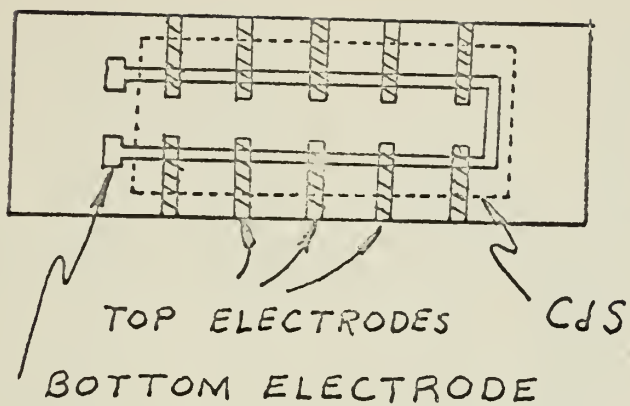


FIGURE 1

$V-i$ CHARACTERISTICS
OF 2145

$d \rightarrow$

1 V/cm HORIZONTAL
 10 ma/cm VERTICAL

$e \rightarrow$

$f -$

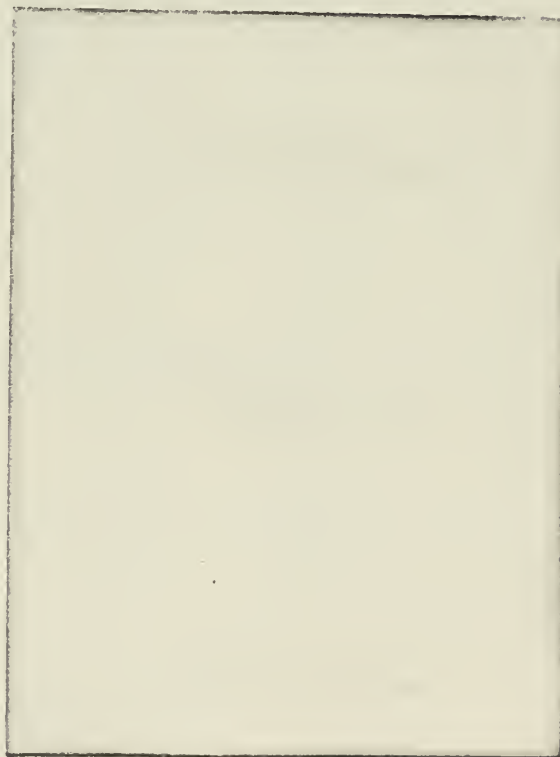
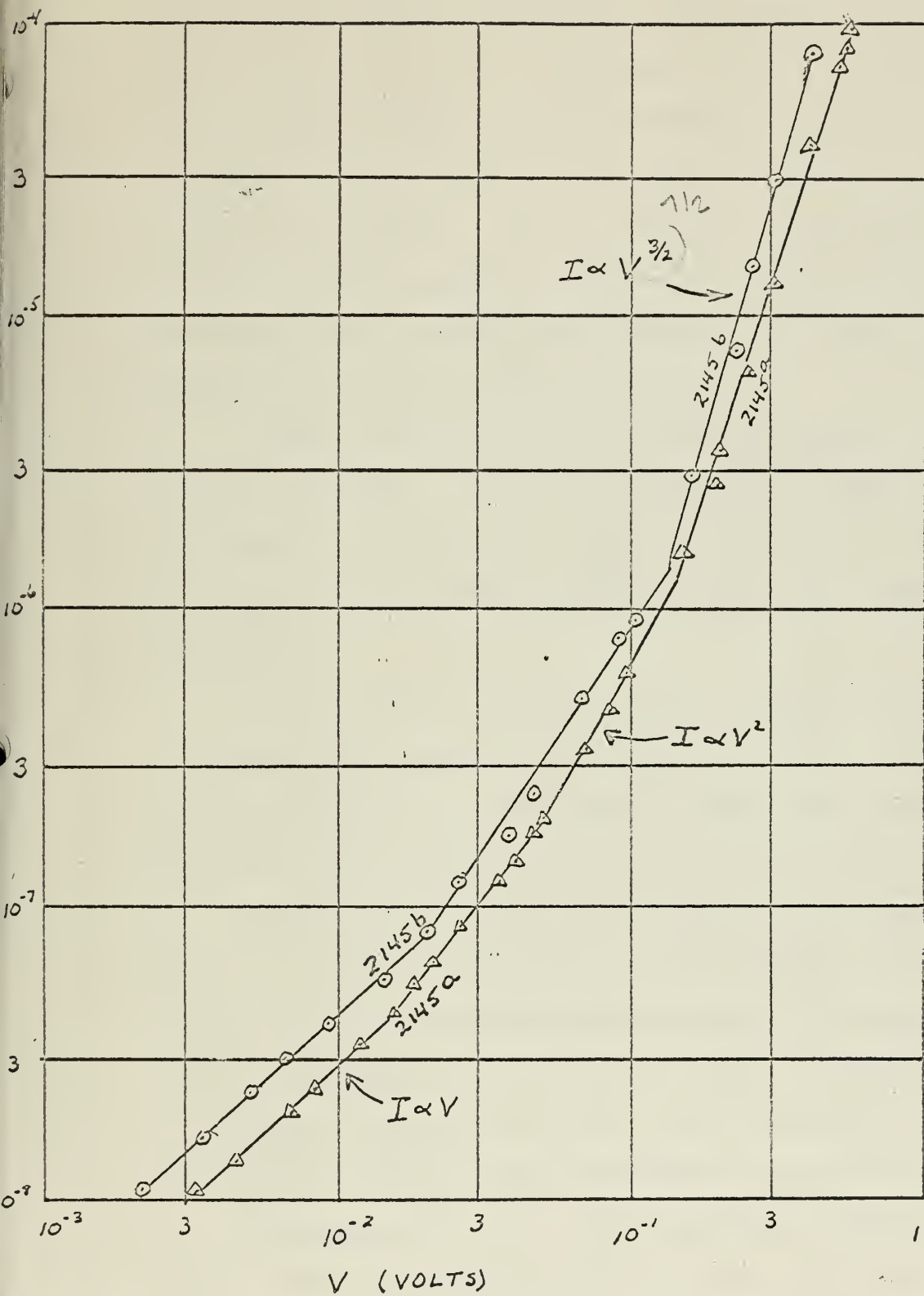


FIGURE 2



I-V CHARACTERISTICS 2145
 FORWARD CURRENT

FIGURE 3

and gold for the top electrode. The cadmium sulfide was evaporated onto a cold substrate and then annealed in vacuum for 20 minutes prior to the addition of the gold. The average thickness of the film as determined by optical interference methods was 1120°\AA . All ten diodes had rectifying properties similar to those shown in figure 2. In all cases the gold electrode was the anode for forward conduction. The cadmium sulfide was markedly photosensitive.

Figure 3 shows static i - v characteristics obtained from 2145a and 2145b. Notice that a region of ohmic dependence followed by a square-law region was observed. Above this, however, a region of $I \propto V^{7/2}$ was observed. This is not easily explained.

Sample 2146 was constructed as nearly 2145 as possible. No non-linear characteristics were observed. The measured average thickness of the cadmium sulfide was 1160°\AA . The maximum observed deviation from this thickness was 180°\AA .

Sample 2154 was made with two gold electrodes. The last 20% of the bottom electrode and the initial part of the cadmium sulfide were evaporated simultaneously to produce a region of forced diffusion. No attempt was made to determine the exact thickness of this mixed layer. Some rectifying characteristics were noted with the bottom electrode positive for forward bias.

In sample 2166, the electrodes were again aluminum and gold. When the sample was first made, a-c characteristics were photographed from the oscilloscope plot. All diodes

and gold for the low albedo. The results indicate an
 overestimated value of 0.05 for the albedo of the
 for 20 albedo values in the range of 0.05. The average
 thickness of the film is estimated to be 100 nm.
 thickness was 120 nm. The total and scattering properties
 similar to those shown in Figure 2. The film was 100 nm
 thickness and the results are shown in Figure 2. The results
 indicate that the film is 100 nm thick.

Figure 3 shows the results of the measurements. The
 120 nm and 100 nm. The results show a range of 100 nm
 followed by a range of 100 nm. The results show a range of 100 nm
 however, a range of 100 nm. The results show a range of 100 nm
 explained.

Figure 4 shows the results of the measurements. The
 120 nm and 100 nm. The results show a range of 100 nm
 followed by a range of 100 nm. The results show a range of 100 nm
 however, a range of 100 nm. The results show a range of 100 nm
 explained.

Figure 5 shows the results of the measurements. The
 120 nm and 100 nm. The results show a range of 100 nm
 followed by a range of 100 nm. The results show a range of 100 nm
 however, a range of 100 nm. The results show a range of 100 nm
 explained.

Figure 6 shows the results of the measurements. The
 120 nm and 100 nm. The results show a range of 100 nm
 followed by a range of 100 nm. The results show a range of 100 nm
 however, a range of 100 nm. The results show a range of 100 nm
 explained.

Figure 7 shows the results of the measurements. The
 120 nm and 100 nm. The results show a range of 100 nm
 followed by a range of 100 nm. The results show a range of 100 nm
 however, a range of 100 nm. The results show a range of 100 nm
 explained.

Figure 8 shows the results of the measurements. The
 120 nm and 100 nm. The results show a range of 100 nm
 followed by a range of 100 nm. The results show a range of 100 nm
 however, a range of 100 nm. The results show a range of 100 nm
 explained.

Figure 9 shows the results of the measurements. The
 120 nm and 100 nm. The results show a range of 100 nm
 followed by a range of 100 nm. The results show a range of 100 nm
 however, a range of 100 nm. The results show a range of 100 nm
 explained.

Figure 10 shows the results of the measurements. The
 120 nm and 100 nm. The results show a range of 100 nm
 followed by a range of 100 nm. The results show a range of 100 nm
 however, a range of 100 nm. The results show a range of 100 nm
 explained.

indicated that gold was the anode for forward current. Several days later, after 2166a was held at 13 volts a-c for several minutes, it was noticed that aluminum had become the anode for forward currents. It was suspected that high fields caused the change.

When 2167 was made, all of the diodes had aluminum as the anode. This raised the possibility of an oxide film effect since it is well known that aluminum oxidizes rapidly even at pressures of 10^{-5} torr. It was also noted that the current remained small until the voltage was approximately one volt. Then the current increased rapidly with increasing voltage. When 7 volts a-c was applied, this slide became too hot to touch. No such heating effects were noticed on any other sample.

The results of 2167 suggested making a diode with the aluminum electrode purposely oxidized in varying amounts to determine the effect of oxide thickness. 2168 was constructed with two diodes anodized to each of the following voltages in a pH 3.0 solution of tartaric acid: 0, 1, 2, 3, and 4 volts. Figure 4 shows the variation of the a-c characteristics with oxide thickness. Notice that the thicker the oxide, the higher the voltage threshold in the forward direction.

The Fowler-Nordheim equation for field emission is well known and may be given by the approximate expression:¹²

$$J = I(\mathcal{E}) \exp \left[\frac{-8\pi}{3h} (2me)^{1/2} \frac{\varphi^{3/2}}{\mathcal{E}} \right] \quad (1)$$

indicated that both the low and high pressure regions were well defined. The low pressure region was found to be at a pressure of 10⁻² mm Hg. and the high pressure region at 10⁻¹ mm Hg. The results are shown in Figure 1. The low pressure region is well defined and the high pressure region is also well defined. The results are shown in Figure 1.

When the pressure was increased from 10⁻² mm Hg. to 10⁻¹ mm Hg. the rate of reaction increased. This is shown in Figure 2. The rate of reaction increased with increasing pressure. This is shown in Figure 2. The rate of reaction increased with increasing pressure. This is shown in Figure 2.

The results of the experiments are shown in Figure 3. The rate of reaction increased with increasing pressure. This is shown in Figure 3. The rate of reaction increased with increasing pressure. This is shown in Figure 3.

The results of the experiments are shown in Figure 4. The rate of reaction increased with increasing pressure. This is shown in Figure 4. The rate of reaction increased with increasing pressure. This is shown in Figure 4.

$$(1) \quad \tau = 1(3) \exp \left[\frac{E}{RT} \right] \quad (2)$$

VARIATION OF I-V
CHARACTERISTICS WITH
DE THICKNESS

2168

1/cm HORIZONTAL
1/cm VERTICAL

3V
2V
1V
VOLTS ANODIZATION

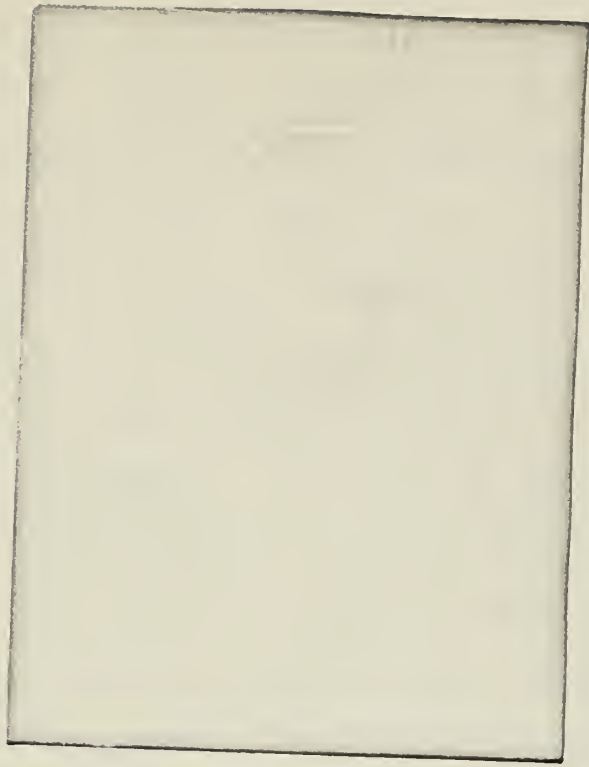


FIGURE 4

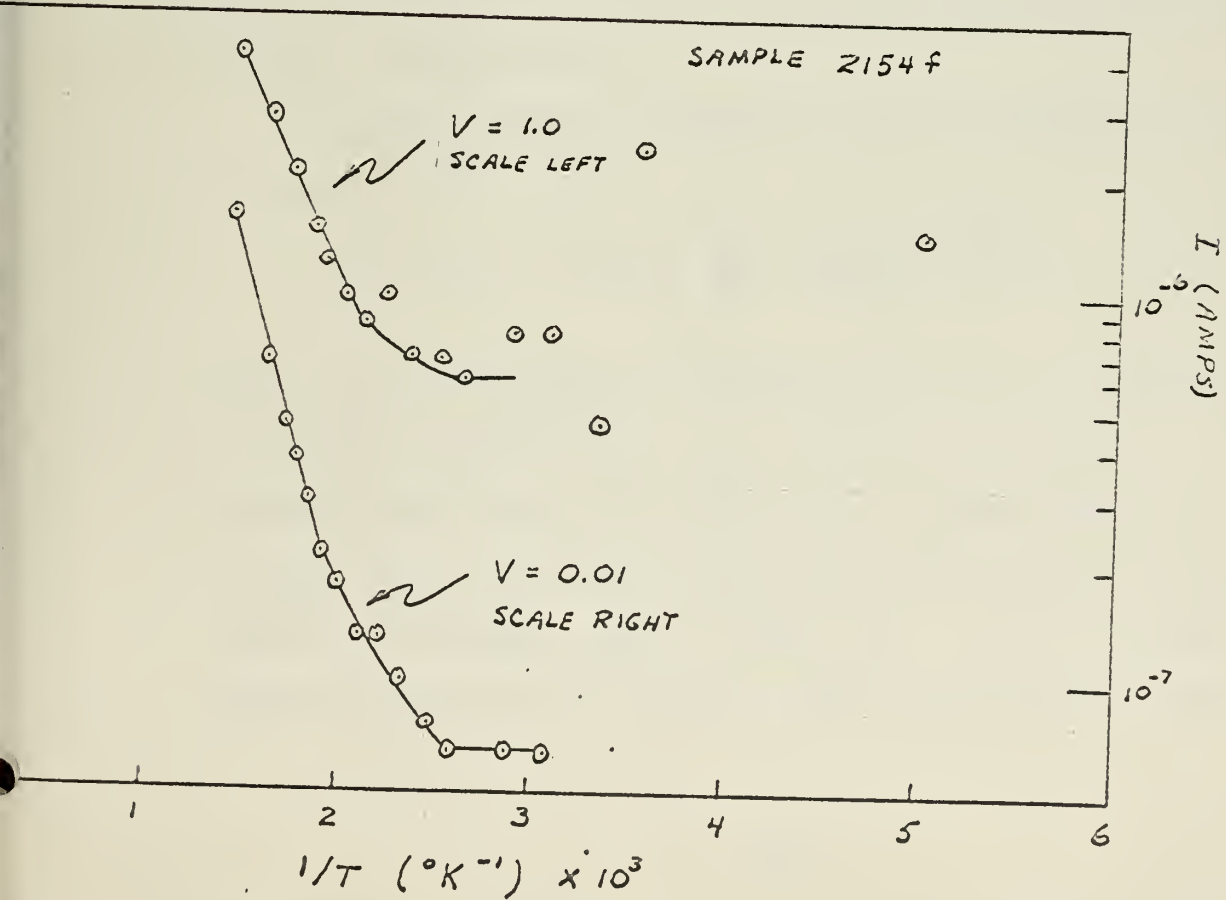


FIGURE 5

$$J \approx I(E) \exp \left[-6 \times 10^9 \frac{\phi^{3/2}}{E} \right] \quad (2)$$

where $I(E) = 1.55 \times 10^{-6} E^2 / \phi$, E is the electric field strength in volts / meter, ϕ is the work function in electron volts. As can be seen from (1), E must be quite large before any appreciable current will flow. However, once this threshold field is reached, the current may be expected to increase as E^2 . This appears to be the case in figure 4.

The current was measured as a function of temperature with the voltage as a parameter for samples 2134c, 2134d, 2154f, and 2154g. The results of these are shown in figure 5. A region of the curve exhibits an essentially temperature independent portion located below a critical temperature. In an effort to determine whether Schottky emission was present, a curve of $\log [(I - I_0) / T^2]$ versus $1/T$ was plotted and is shown in figure 6. (I_0 is the constant current below the critical temperature.)

Schottky emission current-voltage-temperature relation is given by:¹³

$$J = R T^2 \exp \left[\frac{\phi}{k} - C \left(\frac{V}{K a} \right)^{1/2} \right] / T \quad (3)$$

where R is Richardson's constant, ϕ the work function, K the dielectric permittivity, and a the film thickness. C is a constant whose value is 4.389 for V in volts and a in centimeters. From (3) it is evident that the curves of figure 6 should be straight lines as they are. It would appear that Schottky emission was present above the critical temperature.

FIGURE 6

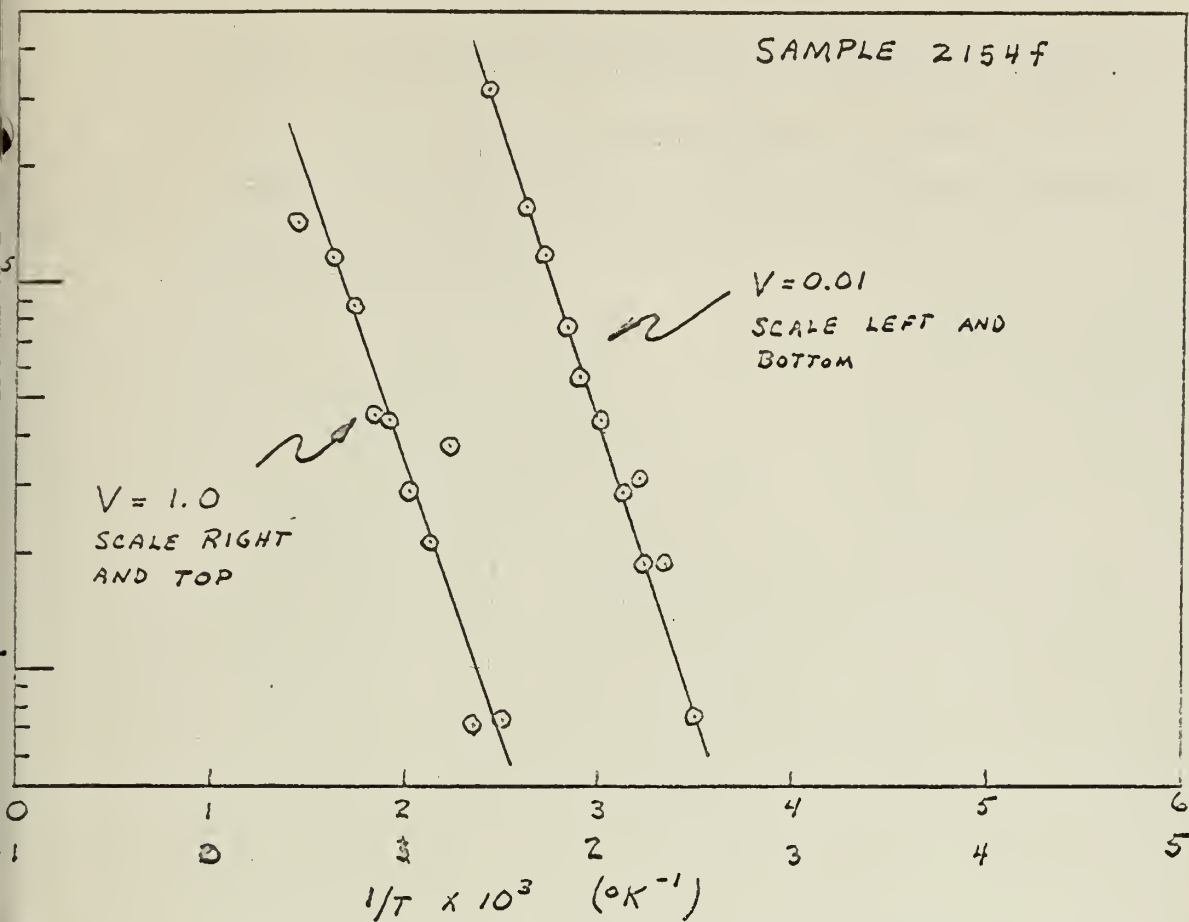
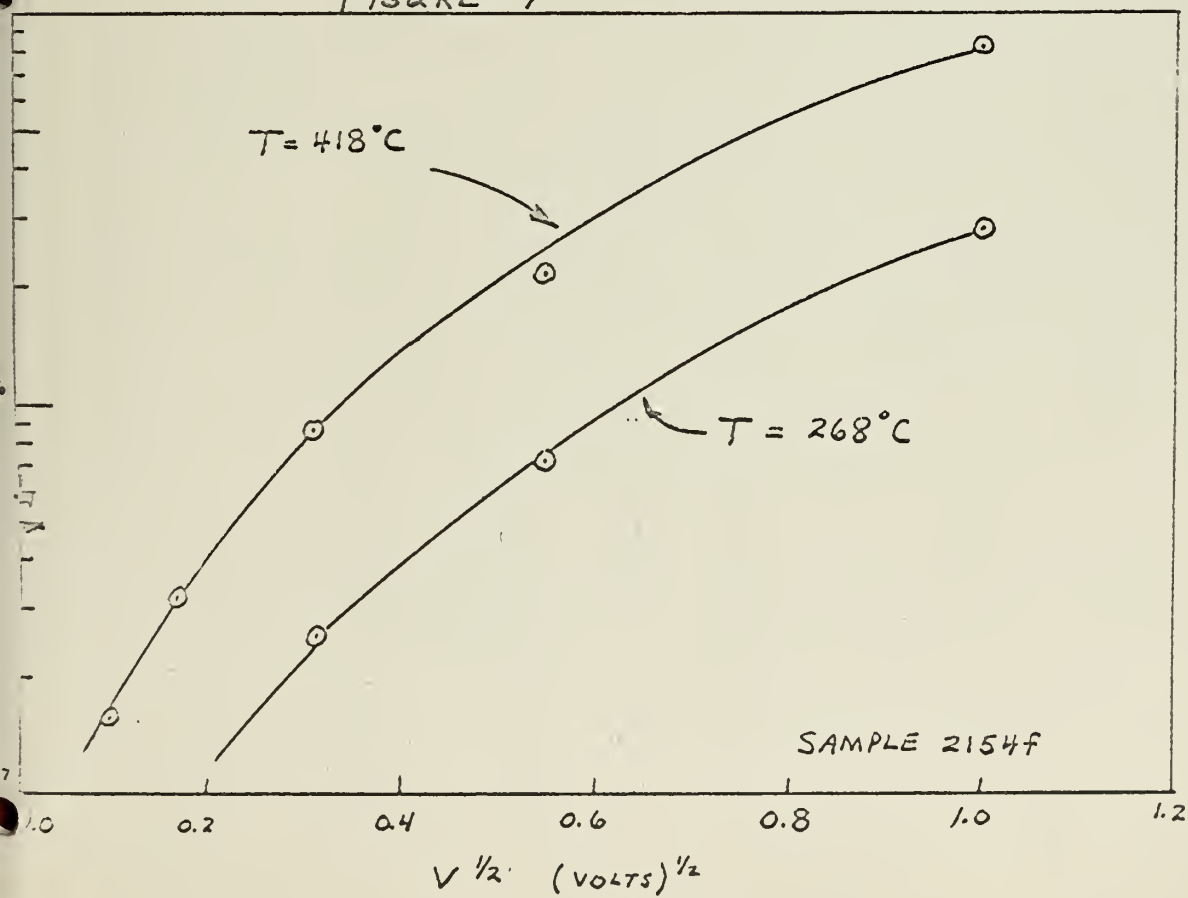


FIGURE 7



This case differs from field emission in that it is temperature dependent and does not set in until some elevated temperature is reached. The field emission data was measured at room temperature.

This work differs from that of the other authors in that it is a
study of the general principles of the science of the earth and
its history. The study of the earth and its history is a
science of the earth and its history.

III. DISCUSSION

Dresner and Shallcross⁸ have pointed out the difficulties of explaining the current process as a space-charge-limited phenomenon. This author found one difficulty they did not mention. The current varying as the $7/2$ power of the voltage in the high current region is difficult to explain using scl currents. Ross¹ has shown that it is possible to obtain $I \propto V (T_0/T + 1)$ for an exponential distribution of traps with energy, but Dresner and Shallcross did not observe such a distribution. A rough calculation by this author based on assuming an impulse distribution of traps at .35 eV below the conduction band gave a square law dependence. Let us follow through this calculation.

We know that the density of trapped electrons, n_t , is given by

$$n_t = \frac{N_t}{1 + \frac{N_c}{n} e^{-E_t/kT}} \quad (4)$$

where N_t is the density of trapping states located E_t below the conduction band. For the approximation given in equation (26), Appendix to hold, we must have

$$\frac{N_c}{n} \gg \exp(E_t/kT) \quad (5)$$

If (5) is true, then (26), Appendix is true, and as the results in the Appendix show, J must then be proportional to V^2 . We can demonstrate that (5) is true for the present

problem.

For the drift limited approximation,

$$J = ne\mu E = \text{constant.} \quad (6)$$

Lampert² has shown that the maximum deviation of E from the average field strength $|E|$ is at most a factor of two. Therefore, we can use (6) together with the experimentally observed values of J and $|E|$ to get the maximum value of J . In our case $J_{\max} \approx 10^{-1}$ amps/cm² with $|E|_{\max} \approx 10^6$ volts/cm. If we assume a mobility of 4 cm/volt-sec, then n is approximately 10^{11} /cm³. $N_0 = 10^{19}$ at room temperature which gives $N_0/n \approx 10^8$. $\exp(E_t/kT) = \exp(40 \times 35) \approx 10^6$. Therefore (5) holds and J should be proportional to V^2 .

We can demonstrate that we have chosen the worst possible case; ie, the case where (5) is the least likely to be valid. If (5) holds for the maximum J , then it must hold for all smaller J values because from (6), n would be even smaller. If μ is larger than the small value (judging from normal values measured in single crystals), then again n is smaller. Therefore, we conclude that J should be proportional to V^2 and should not have a $J \propto V^{7/2}$ range which was observed.

We can make a few remarks about using the exponential trap distribution of Rose. First, as we mentioned above, the measured trapping density was not exponential. Second, we can show that if the exponential distribution does hold, then at constant voltage, current should increase with decreasing temperature. We will use Rose's¹ calculations, but will fill

in the constant he did not state except to say that it was a function of temperature. Rose defined

$$n_t = A \exp(-E_t / k T_c) \quad (7)$$

where A is a constant and the other symbols are as before. The condensed charge forced into the insulator is

$$Q = CV \quad (8)$$

where C is the capacitance. This condensed charge raises the Fermi level by an amount E defined by the relation

$$\int_{E_f - \Delta E}^{E_f} A \exp(-E_t / k T) dE = \frac{CV}{e} \quad (9)$$

The solution of this equation (neglecting the upper limit) is:

$$\Delta E = k T_c (\ln V + K) \quad (10)$$

where

$$K = \ln \left(\frac{C}{AekT_c} \right) + \frac{E_f}{kT_c} \quad (11)$$

If we define Θ as the ratio of free to total charge, we can write

$$\Theta = \frac{eN_c}{CV} \exp \left(-E_f / kT + \Delta E / kT \right) \quad (12)$$

where N_c is the effective density of states in the conduction band. If we use (10) for E , then

$$\Theta = \frac{eN_c}{CV} \left[V \frac{T_c}{T} \left(\frac{C}{AekT_c} \right)^{T_c/T} \right] \quad (13)$$

is the number of the atoms in the system, N , and k is the Boltzmann constant.

$$(7) \quad \left(\frac{\partial}{\partial T} \ln Z \right)_{N, V} = \frac{U}{kT^2}$$

where U is the internal energy of the system, and Z is the partition function.

$$(8) \quad Q = \frac{1}{N!} \int \exp(-\beta H) d\mathbf{r}^N d\mathbf{p}^N$$

where Q is the partition function, H is the Hamiltonian, \mathbf{r}^N and \mathbf{p}^N are the coordinates and momenta of the N particles.

$$(9) \quad \frac{Q}{Q_0} = \frac{1}{N!} \int \exp(-\beta H) d\mathbf{r}^N d\mathbf{p}^N$$

where Q_0 is the partition function of the ideal gas, and H is the Hamiltonian.

$$(10) \quad \Delta E = kT \ln \left(\frac{Z}{Z_0} \right)$$

where

$$(11) \quad \frac{1}{kT} = \frac{1}{kT_0} + \left(\frac{\partial}{\partial E} \ln Z \right)_{N, V}$$

It is defined as the inverse of the temperature, $1/kT$, and Z is the partition function.

$$(12) \quad \left(\frac{\partial}{\partial T} \ln Z \right)_{N, V} = \frac{U}{kT^2}$$

where U is the internal energy of the system, and Z is the partition function. It is used in the derivation of the equation of state.

$$(13) \quad \left(\frac{\partial}{\partial T} \ln Z \right)_{N, V} = \frac{U}{kT^2}$$

We now use equation (25) from the Appendix which may be written as

$$J = \frac{q}{8} \frac{\epsilon_0 \mu}{d^3} V^2 \quad (14)$$

It can be seen from equation (22), the appendix that the in (14) is the same as (13). Therefore we have

$$J = (\text{constant}) V^{\frac{T_c}{T} + 1} \left(\frac{C}{A e k T_c} \right)^{\frac{T_c}{T}} \quad (15)$$

which verifies our statement that the current increases with decreasing temperature. This was not observed experimentally. On the contrary, the opposite effect was noted.

From the two calculations we have just made, we must conclude that space-charge-limited currents alone cannot explain the experimentally observed facts. We must seek other physical processes to explain the data. Two which came to mind were field emission and Schottky emission.

Field emission seemed a likely candidate when it was noted that the diodes had a very sharp voltage threshold for conduction with the aluminum positive. The Fowler-Nordheim equation is given by (2). If we assume an oxide thickness of 10^9 \AA which we postulate as having been inadvertently created on the aluminum electrode during the manufacturing process, we can demonstrate that a voltage threshold would exist. For $E < 10^7$ volts/cm, the exponential term in (2) is vanishingly small. As a matter of fact, E must be of the order of 10^8 volts/cm before the current density approaches 10^{-6} amps/cm². A field of 10^8 volts/cm in the present case corresponds to a

the two cases considered (1) and (2) the conductivity is not the same
 but the

$$I = \frac{q}{8} \sqrt{\frac{2}{\pi}} \sqrt{\frac{2}{\pi}}$$

(2)

it can be seen from equation (1) that the conductivity is
 in (1) is the same as (2), therefore we have

$$I = (\text{const}) \sqrt{\frac{2}{\pi}} \sqrt{\frac{2}{\pi}} \left(\frac{q}{8} \sqrt{\frac{2}{\pi}} \right)^{\frac{1}{2}}$$

which verifies our statement that the conductivity is
 decreasing exponentially. This was the expected result.
 In the literature, the typical effect was noted.

From the two calculations we have seen that the
 conductivity is proportional to the square root of the
 grain size. This is a very important result. It shows that the
 physical processes are similar in the two cases. The result was
 also seen from the conductivity and density analysis.

This analysis shows a likely condition when it was
 noted that the density had a very sharp change. This is
 consistent with the atomic position. The conductivity
 analysis is given by (2). It is shown in figure 1 that
 at 10^6 which is consistent with having been experimentally measured
 for the minimum electrode during the annealing process.
 we can demonstrate that a voltage threshold would exist. For
 10^6 voltage, the exponential term in (1) is sufficiently
 small. In a matter of fact, it is of the order of 10^6
 voltage before the current density approaches 10^6 amp/cm².
 A field of 10^6 volt/cm in the present case corresponds to a

terminal voltage of 1 volt providing all of the field is across the oxide.

The results obtained by purposely oxidizing the aluminum show conclusively that oxide does have an effect on the current characteristics. However, the results are insufficient to show indisputably that field emission is present. Instead, we can only remark that the observed shifting of the voltage threshold value with increased oxide thickness is indicative of field emission and the the magnitude of this threshold is approximately correct,

We can make a fairly strong case for Schottky emission. Figure 5 indicates a definite temperature dependance of the current above a certain critical temperature. Below this critical temperature, the current is relatively temperature independent. This type of behavior is suggestive of Schottky emission. Reference to (3) shows that if Schottky emission is the dominant physical process we should expect plots of $\log I$ versus $V^{\frac{1}{2}}$ and $\log [(I-I_0)/T^2]$ versus $1/T$ to be straight lines. These plots are shown in figures 6 and 7. In figure 6, we see that we have a fairly straight line, especially at higher values of T (lower values of $1/T$). The erratic part of the line tends to be at the low temperature end. This is because at this end of the curve, I_0 played a significant role. Any inaccuracy in the determination of I_0 would affect the curve radically. At the other end, however, I_0 was almost negligible in comparison with I and hence, any inaccuracy in

Figure 2 indicates a definite dependence of the
current upon a certain critical temperature. Below this
critical temperature, the current is relatively independent
of temperature. This type of behavior is characteristic of
superconductors. According to (1) it seems that the observed
behavior of the current is due to the presence of a
critical temperature T_c and for $T < T_c$ the current
is zero. These data are shown in Figure 1 and 2. In Figure
1 we see that we have a fairly sharp jump, especially at
higher values of T (lower values of I). The critical
temperature T_c seems to be at the low temperature end. This is
evident at this end of the curve. It plays a significant role
in the determination of the critical temperature. At the other end, however, it was almost
negligible in comparison with T and hence any influence in

It would go unnoticed.

In figure 7, it is difficult to account for the observed curve. As stated above, we expect a straight line if Schottky emission was present. We could not offer any explanation, and for this reason we were unable to conclude that Schottky emission was definitely observed.

The first of these is the fact that the
author is not a native speaker of the
language. He is a native speaker of
English and has learned the language
as a second language. This is a
disadvantage in that he may not be
able to express himself as fluently
as a native speaker. However, he
has made every effort to make his
writing as clear and understandable
as possible.

IV. CONCLUSIONS

In attempting to draw some conclusions from the data, this author was forced to make only a conjecture since conclusive evidence was not available. It is suggested that both field emission and Schottky emission occur in the diode. In the high temperature region, Schottky emission is dominant and in the low temperature region tunneling occurs. Space-charge-limited currents can be ruled out. Further experiments are necessary to pin down definitely the physical processes that were observed.

The experiments that this author considers need to be done are the following:

(a) Make several samples with varying oxide thicknesses and measure i-v characteristics at different temperatures with the purpose of looking for Schottky emission above the critical temperature.

(b) Use a higher vacuum system to attempt to eliminate the inadvertant formation of oxide on the aluminum.

(c) Conduct noise measurements on the sample to obtain further evidence of the lack of space charge current. This situation would be indicated if a failure to observe space charge suppression of noise.

(d) Conduct a thermal determination of density of trapping states.

(e) Measure the capacitance of the samples with different bias values.

APPENDIX

SPACE-CHARGE-LIMITED CURRENTS IN SOLIDS

Space Charge Limited Currents (SCLC) in insulators have been investigated theoretically by a number of workers. The first results of any consequence was the derivation of the Child-Langmuir Law for a trap-free insulator by Mott and Gurney.¹⁵ Following their work, (but using the mathematical convention of Lampert,² et al. that $\vec{E} = -E\hat{x}$, $\vec{J} = -J\hat{x}$, & $E = \frac{dV}{dx}$) we first write the general current flow equation:

$$J = ne\mu E - eD \frac{dn}{dx}, \quad (1)$$

where J is the current density, n is the electron density, e is the magnitude of the electronic charge, μ is the mobility, E is the electric field strength, and D is the diffusion constant for electrons. Then in addition we have Poisson's equation:

$$\frac{dE}{dx} = \frac{ne}{\epsilon}, \quad (2)$$

where ϵ is the dielectric constant of the material.

In an insulator, we assume that the diffusion component of the current is negligible in comparison with the drift component, ie, (1) becomes:

$$J = ne\mu E = \text{constant} \quad (3)$$

THEORY OF THE ELECTRIC FIELD

Let us consider a point charge q located at a distance r from the origin of the coordinate system. The electric field E at a point P is defined as the force F acting on a unit positive charge placed at P . The force F is given by Coulomb's law:

$$F = \frac{1}{4\pi\epsilon_0} \frac{qQ}{r^2} \quad (1)$$

where Q is the charge of the test charge, ϵ_0 is the permittivity of free space, and r is the distance between the charges. The electric field E is a vector quantity, and its direction is the same as the direction of the force F . The magnitude of the electric field E is given by:

$$E = \frac{F}{Q} = \frac{1}{4\pi\epsilon_0} \frac{q}{r^2} \quad (2)$$

where E is the electric field strength at the point P . In an electric field, the force F acting on a charge Q is given by:

$$F = QE \quad (3)$$

If we carry out the integration of (1) and (3) we obtain

$$\mathcal{E} = \pm \left(\frac{2 J x}{\epsilon \mu} + \text{constant} \right)^{1/2} \quad (4)$$

To evaluate the constant we must use an appropriate boundary condition. We assume that this is $\mathcal{E}=0$ at $x=0$. Reference to figure 8 shows that this is equivalent to having the cathode at $x=x_0$. If x_0 is small in comparison with the thickness of the insulator, then the assumption of the boundary condition is valid. The negative sign in (4) may be discarded as is obvious from either (3) or the figure.

To relate the applied voltage to the observed current we integrate (4)

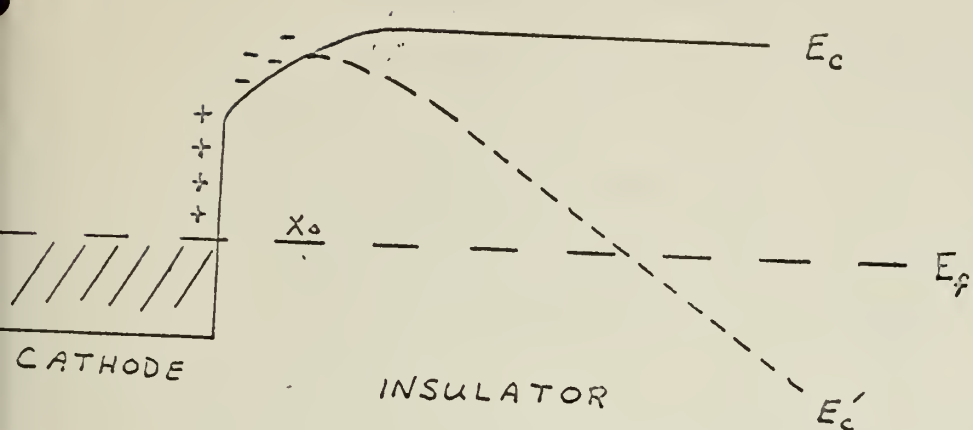
$$V - \frac{\phi_2 - \phi_1}{e} = \int_0^d \mathcal{E} dx = - \frac{2}{3} \left(\frac{2 J}{\epsilon \mu} \right)^{1/2} d^{3/2} \quad (5)$$

or in terms of $i = - JA$ we have

$$i = \frac{9}{8} \frac{\epsilon \mu A}{d^3} (V - V_0)^2 \quad (6)$$

where $V_0 = \frac{\phi_2 - \phi_1}{e}$, ϕ_2 is the work function of the anode, and ϕ_1 is the work function of the cathode. This result is the Child-Langmuir law for solids. We see that it differs from the vacuum law primarily by a factor of V^2 instead of $V^{3/2}$.

This result has several serious difficulties as was pointed out by Lampert₄ and clarified considerably by Lindmayer, Reynolds, and Wrigley. We have assumed that $\mathcal{E}=0$ at $x=0$. But if this is true, then (3) tells us that $J(0)=0$ or $J=0$ everywhere since the current is constant. Also the problem



BAND MODEL OF SPACE-CHARGE-LIMITED CURRENT (AFTER WRIGHT³)

FIGURE 8

SOLUTION OF THE SPACE CHARGE PROBLEM INCLUDING DIFFUSION ACCORDING TO LINDMAYER, REYNOLDS, AND WRIGLEY⁴

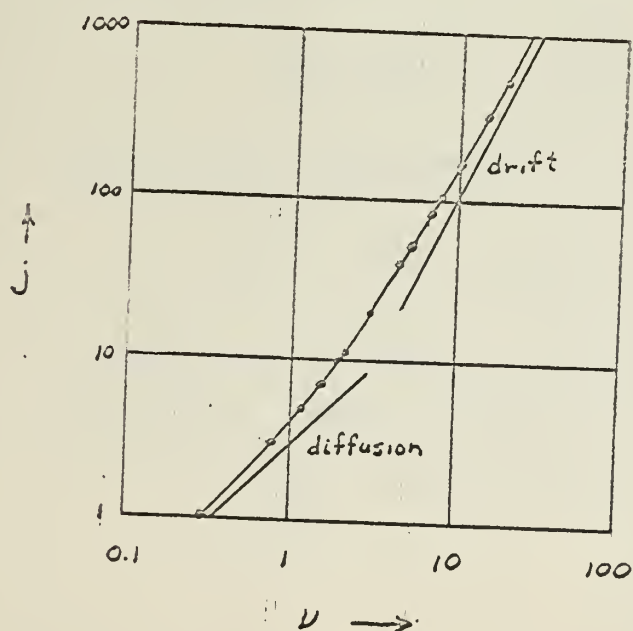


FIGURE 9

has two natural boundary conditions, one at $X=0$ and one at $X=d$. In the above discussion we have only used the one at $X=0$. The trouble comes in neglecting the diffusion current. Lindmayer, et al. have solved the complete problem which we shall give here for convenience.

First let us combine (1) and (2) to obtain

$$J = \epsilon \mu E E' - \epsilon D E'' \quad (7)$$

where the primed quantities indicate differentiation with respect to X . We simplify this equation by the use of the normalizations:

$$\begin{aligned} S &= \lambda/d \\ F &= -\mu d E/D \\ j &= \mu d^3 J / \epsilon D^2 \end{aligned} \quad (8)$$

to obtain:

$$j = F'' + \frac{(F^2)'}{2}. \quad (9)$$

Integrating once

$$Sj + C_1 = F' + \frac{F^2}{2}. \quad (10)$$

Now if the substitution $F = 2u'/u$ is made we have

$$u'' = (C_1 + Sj) u/2 \quad (11)$$

which is an ordinary, linear differential equation. We simplify (11) even farther by making the change of variable

$$z = -(C_1 + Sj) / (2j^2)^{1/3} \quad (12)$$

the two natural numbers m and n are both
 odd. In the above situation it will then be the case
 that the level of the m -th and n -th elements of the
 sequence is the same. The level of the m -th element is
 the same as the level of the n -th element. This is
 still true for the sequence.

Thus we have shown (i) and (ii) to be false.

$$(17) \quad 1 = 1 + 1 + 1 + \dots$$

where the right hand side is the sum of the
 terms of the sequence. The sum of the terms of the
 sequence is the same as the sum of the terms of the
 sequence.

$$(18) \quad \begin{aligned} 1 &= 1 + 1 + 1 + \dots \\ 0 &= 1 + 1 + 1 + \dots \\ 1 &= 1 + 1 + 1 + \dots \end{aligned}$$

to obtain

$$(19) \quad 1 = 1 + 1 + 1 + \dots$$

Substituting

$$(20) \quad 1 = 1 + 1 + 1 + \dots$$

Now if the sequence $F = 1, 1, 1, \dots$ is used we have

$$(21) \quad 1 = 1 + 1 + 1 + \dots$$

which is an obvious contradiction. The contradiction is obvious.
 (ii) even though it seems the case to be false

$$(22) \quad 1 = 1 + 1 + 1 + \dots$$

The result is

$$\frac{d^2 u}{dz^2} + \beta u = 0 \quad (13)$$

This equation has a solution of the form $u = k_1 f_1 + k_2 f_2$ where the k 's are arbitrary constants. As Lindmayer, et al. have pointed out, the apparent three constants are in reality only two. This may be seen by calculating the normalized potential, V ,

$$V = \frac{qV}{kT} = \int_0^1 F ds = 2 \int_0^1 \frac{u'}{u} = 2 \ln \frac{u(1)}{u(0)}, \quad (14)$$

where we have used the Einstein relation $\frac{D}{\mu} = \frac{kT}{q}$. Now putting the general solution into (14) we have the result that

$$V = 2 \ln \left\{ \frac{k_1 f_1(1) + k_2 f_2(1)}{k_1 f_1(0) + k_2 f_2(0)} \right\} = 2 \ln \left\{ \frac{f_1(1) + C_2 f_2(1)}{f_1(0) + C_2 f_2(0)} \right\} \quad (15)$$

It is now apparent that only two constants exist.

The solution to (13) is known in the form of an infinite series and is given by Lindmayer, et al. This solution, however, is not one that allows a straight-forward application of the boundary conditions, since the constants C_1 and C_2 are buried in the series. The boundary conditions may be applied by use of a computer trial and error process. Before we look at the results of this computation, let us determine the appropriate boundary conditions to use.

If we consider a physical structure with a material sandwiched between an anode and a cathode, then the boundary condition at $x=0$ (the anode) or $s=1$ is

$$F'(1) = 0 \quad \text{or} \quad \left. uu'' \right|_{s=1} = \left. (u')^2 \right|_{s=1} \quad (16)$$

$$0 = \frac{1}{2} \frac{d}{dt} \left(\frac{1}{2} \dot{\theta}^2 + \frac{1}{2} \dot{\phi}^2 \right)$$

(12)

This equation is a constant of the motion. It shows that the two angular momenta are constant. This can be seen by differentiating the Hamiltonian with respect to time. The result is zero, which shows that the total angular momentum is conserved.

From the general solution (11) we know that the motion is periodic. The period is given by $T = 2\pi / \omega$, where ω is the frequency of the motion. This can be seen by substituting the general solution into the equations of motion and simplifying.

It is now required that the motion be periodic. This is satisfied if the frequency ω is a rational number. The condition for this is that the ratio of the two frequencies is a rational number.

The condition for (11) to hold is that the motion is periodic. This is satisfied if the frequency ω is a rational number. The condition for this is that the ratio of the two frequencies is a rational number.

The boundary conditions are that the motion is periodic. This is satisfied if the frequency ω is a rational number. The condition for this is that the ratio of the two frequencies is a rational number.

It is now required that the motion be periodic. This is satisfied if the frequency ω is a rational number. The condition for this is that the ratio of the two frequencies is a rational number.

$$F(\omega) = 0 \quad \text{or} \quad \omega = 0$$

if we assume that all electrons arriving at the anode are swept away by the field.

The boundary conditions at $X=0$ or $S=0$ is less apparent. We first assume that the electric field here is equal to zero. We see that since we have included the diffusion component of the current as well as the drift component, this boundary condition no longer leads to zero current as previously. Hence, we take as our second boundary condition

$$F(0) = 0 \quad \text{or} \quad u \frac{dF}{dS} \bigg|_{S=0} = 0 \quad (17)$$

The results obtained by Lindmayer, Reynolds, and Wrigley are shown in figure 9.

Let us examine these results in more detail. When the current (or j) is low, then we assume a diffusion limited situation. If this is so then (9) becomes

$$j = F_j'' \quad (18)$$

which has a solution

$$j = 3u \quad (19)$$

Figure 9 shows this solution plotted in comparison with the complete solution. Also shown is the drift limited case.

Calculating the transition for high values of j is difficult. Lindmayer, et al. found that $f_1(0)$ and $C_2 f_2(0)$ in (15) form a difference with variation only in the eighth significant figure for values of $j > 600$. But by calculating F

All the functions have the same period as the function f .
 Hence we may say that f is periodic.

The following conditions are satisfied by f in case (1).

We have shown that the function f has the same period as f .
 We now show that the function f has the same period as f .
 The function f has the same period as f .
 We have shown that the function f has the same period as f .
 We have shown that the function f has the same period as f .

$$(12) \quad f(x) = 0 \quad \text{for } x \in \mathbb{R}$$

The function f has the same period as f .
 Hence we may say that f is periodic.

We have shown that the function f has the same period as f .
 We have shown that the function f has the same period as f .
 We have shown that the function f has the same period as f .

$$(13) \quad f(x) = 0 \quad \text{for } x \in \mathbb{R}$$

Hence we may say that f is periodic.

$$(14) \quad f(x) = 0 \quad \text{for } x \in \mathbb{R}$$

Figure 1 shows the function f in case (1).
 complete solution. This shows that the function f has the same period as f .
 Calculating the derivative for the value of f in case (1).
 Hence we may say that f is periodic.
 Hence we may say that f is periodic.
 Hence we may say that f is periodic.

point by point and starting at both boundaries, they were able to project the curve to $j=10^4$. Up to this limit the series solution appears to be approaching the drift limited case. The error is below 10% in the drift limited approximation for $V > 100 kT/g$.

The work of Lindmayer, et al. appears to give justification for our previous assumption that the diffusion current could be neglected as long as $V > 100 kT/g$ in the case of a trap-free structure. We shall assume that it is likewise justified to make the same assumption in the case of trapping. If we neglect diffusion, then the equations we must solve are:

$$\frac{dE}{dx} = \frac{(n+n_t)e}{\epsilon} \quad (20)$$

$$J = ne\mu E \quad (21)$$

where n is the density of free carriers, n_t is the density of trapped carriers, and the other symbols are as before. If we define

$$\Theta \equiv \frac{n}{n+n_t} \quad (22)$$

and substitute for $n + n_t$ in (20) we have

$$\frac{\epsilon\Theta}{e} \frac{dE}{dx} = n \quad (23)$$

which may be substituted into (21) which gives:

$$J = e\mu\Theta E \frac{dE}{dx} \quad (24)$$

If Θ is independent of x , then the solution of (24) is

... the ... of the ...
 ... the ... of the ...
 ... the ... of the ...
 ... the ... of the ...
 ... the ... of the ...

The ... of the ...
 ... the ... of the ...
 ... the ... of the ...
 ... the ... of the ...
 ... the ... of the ...

$$(12) \quad \frac{3(2x + 1)}{2} = \frac{3b}{2}$$

$$(13) \quad 3x + 1 = T$$

... the ... of the ...
 ... the ... of the ...
 ... the ... of the ...

$$(14) \quad \frac{F}{m} = 0$$

... the ... of the ...
 ... the ... of the ...
 ... the ... of the ...

$$(15) \quad F = \frac{3b}{2} \frac{3b}{2}$$

$$(16) \quad \frac{3b}{2} \frac{3b}{2} = T$$

... the ... of the ...
 ... the ... of the ...
 ... the ... of the ...

the same as (6) with $\Theta\mu$ substituted for μ or

$$i = \frac{9}{8} \frac{\epsilon \Theta \mu A}{d^3} (V - V_0)^2. \quad (25)$$

Θ is given approximately by

$$\Theta = \frac{N_c}{N_t} \exp(-E_t/kT) \neq \Theta(x) \quad (26)$$

for the case of a single level of shallow traps whose density is N_t and whose distance below the conduction band is E_t . N_c is 10^{19} at room temperature. For $N_t = 10^{17}$ and $E_t = 0.5$ volt, $\Theta = 10^{-7}$ and space-charge-limited currents are greatly reduced.

In general, we cannot assume $\Theta \neq \Theta(x)$ as was done above. The exact mathematical solution becomes very complicated if not impossible to carry out. Before we attempt to do more with the solution, let us examine some of the characteristics of the problem and see what can be learned without a rigorous solution.

The problem we are solving is the set of equations (20) and (21) plus the fact that we assume n and n_t are specified by the normal Fermi statistics. We can write the equation relating $n(x)$ to E_F , the Fermi energy as:

$$n(x) = N_c \exp\{[E_F(x) - E_c(x)]/kT\} \quad (27)$$

where N_c is the effective density of states in the conduction band at temperature T and $E_c(x)$ is the lower edge of the conduction band. When a set of traps of density N_t at energy $E_t(x)$ are in quasi-equilibrium with $n(x)$, then

$$1 = \frac{1}{8} \frac{d^2 \phi}{dx^2} (1 - \phi)$$

(12)

THE JOURNAL OF THE AMERICAN MEDICAL ASSOCIATION

$$\phi = \frac{1}{8} \frac{d^2 \phi}{dx^2} (1 - \phi)$$

(13)

For the case of a small angle of deflection the solution of the differential equation (12) is $\phi = \frac{1}{8} \frac{d^2 \phi}{dx^2} (1 - \phi)$ and the solution of the differential equation (13) is $\phi = \frac{1}{8} \frac{d^2 \phi}{dx^2} (1 - \phi)$. The solution of the differential equation (14) is $\phi = \frac{1}{8} \frac{d^2 \phi}{dx^2} (1 - \phi)$.

The solution of the differential equation (15) is $\phi = \frac{1}{8} \frac{d^2 \phi}{dx^2} (1 - \phi)$. The solution of the differential equation (16) is $\phi = \frac{1}{8} \frac{d^2 \phi}{dx^2} (1 - \phi)$. The solution of the differential equation (17) is $\phi = \frac{1}{8} \frac{d^2 \phi}{dx^2} (1 - \phi)$. The solution of the differential equation (18) is $\phi = \frac{1}{8} \frac{d^2 \phi}{dx^2} (1 - \phi)$.

The solution of the differential equation (19) is $\phi = \frac{1}{8} \frac{d^2 \phi}{dx^2} (1 - \phi)$. The solution of the differential equation (20) is $\phi = \frac{1}{8} \frac{d^2 \phi}{dx^2} (1 - \phi)$. The solution of the differential equation (21) is $\phi = \frac{1}{8} \frac{d^2 \phi}{dx^2} (1 - \phi)$. The solution of the differential equation (22) is $\phi = \frac{1}{8} \frac{d^2 \phi}{dx^2} (1 - \phi)$.

$$(23) \quad \phi = \frac{1}{8} \frac{d^2 \phi}{dx^2} (1 - \phi)$$

where ϕ is the deflection angle of the beam at the end of the beam. The solution of the differential equation (24) is $\phi = \frac{1}{8} \frac{d^2 \phi}{dx^2} (1 - \phi)$. The solution of the differential equation (25) is $\phi = \frac{1}{8} \frac{d^2 \phi}{dx^2} (1 - \phi)$. The solution of the differential equation (26) is $\phi = \frac{1}{8} \frac{d^2 \phi}{dx^2} (1 - \phi)$.

$$\begin{aligned} n_t(x) &= N_t \left\{ 1 + \exp \left([E_t(x) - E_f(x)] / kT \right) \right\}^{-1} \\ &= n(x) N_t \{ n(x) + N \}^{-1} \end{aligned} \quad (28)$$

with $N = N_c \exp \{ [E_t(x) - E_c(x)] / kT \}.$

The boundary condition we assume is as before $E=0$ at $x=0$.

Following Lampert we can make some very general observations about the set of equations. In the neutral crystal, (ie, no injected charge) ohm's law must hold. This follows because Poisson's equation becomes

$$\frac{dE}{dx} = 0, \quad (29)$$

but since J is a constant,

$$\frac{dJ}{dx} = 0 = ne\mu \frac{dE}{dx} + e\mu E \frac{dn}{dx} \quad (30)$$

The first term on the right in (30) is zero from (29). Therefore, the second term on the right is zero. This implies $dn/dx=0$ or $n=n_0$ is a constant independent of x . We may then define $ne\mu = \sigma$ and Ohm's law results.

Ohm's law and Child's law curves intersect when the excess injected carrier density at the anode calculated from Child's law becomes similar to n_0 , the neutral carrier density. We can find the voltage, V_a , at which the crossover occurs by equating the ohmic current to the space-charge-limited current,

$$J_a = en_0\mu \frac{V_a}{d} = J_{scl} = \frac{9}{8} \frac{\epsilon\mu}{d^3} V_a^2 \quad (31)$$

which gives

$$\{ (T+1)(\omega_2 - \omega_1) \} \{ 9 \times 10^9 + 1 \} \{ V = (0, 0) \}$$

$$\{ 11 + 10 \times 10^9 \} \{ V = (0, 0) \}$$

$$\{ 7 \times 10^9 (1 - 10^{-10}) \} \{ V = (0, 0) \}$$

The following is a list of the values of the various quantities.

100

Following is a list of the values of the various quantities. The values are given in units of 10^9 for the first three quantities, and in units of 10^{10} for the last two quantities. The values are given in units of 10^9 for the first three quantities, and in units of 10^{10} for the last two quantities.

$$\alpha = \frac{3b}{\lambda b}$$

100

The following is a list of the values of the various quantities.

$$\frac{3b}{\lambda b} \{ 3 \times 10^9 + 1 \} \{ V = (0, 0) \} = 0 = \frac{1b}{\lambda b}$$

100

The following is a list of the values of the various quantities. The values are given in units of 10^9 for the first three quantities, and in units of 10^{10} for the last two quantities. The values are given in units of 10^9 for the first three quantities, and in units of 10^{10} for the last two quantities.

The following is a list of the values of the various quantities. The values are given in units of 10^9 for the first three quantities, and in units of 10^{10} for the last two quantities. The values are given in units of 10^9 for the first three quantities, and in units of 10^{10} for the last two quantities.

$$\{ 11 + 10 \times 10^9 \} \{ V = (0, 0) \}$$

100

100

$$V_a = \frac{g}{q} \frac{e n_o d^3}{\epsilon} . \quad (32)$$

Let us now examine the situation when all of the traps within the insulator are filled. We shall find that this gives us a third limit on our J-V characteristics.

When all of the traps are filled, then there is an un-neutralized charge present in the insulator that tends to prevent additional charge injection. The voltage is necessary to overcome the repulsion from the charge condensed in the traps. Let us follow the mathematics through for this case in more detail.

If all of the traps are filled, then $n_t = N_t$ and Poisson's equation becomes

$$\frac{dE}{dx} = (n + N_t) \frac{e}{\epsilon} . \quad (33)$$

We now substitute (33) in (30) and use () to obtain a non-linear differential equation in n as

$$\frac{dn}{dx} + n^3 \frac{e^2 u}{\epsilon J} + n^2 \frac{N_t e^2 u}{J} = 0 \quad (34)$$

This equation is separable and the integral in n is tabulated.

Using the boundary condition that at $x=0$ gives

$$x = \left(\frac{\epsilon J}{N_t e^2 u} \right) \frac{1}{n} - \left(\frac{\epsilon J}{N_t^2 e^2 u} \right) \ln \left(1 + \frac{N_t e^2 u}{\epsilon J} \right) \quad (35)$$

or with n eliminated,

$$x = \frac{\epsilon}{e N_t} - \frac{\epsilon J}{e^2 N_t^2 u} \ln \left(1 + \frac{e N_t u}{J} \epsilon \right) . \quad (36)$$

$$0 = \frac{a^2 b^2}{L^2} \pi^2 + \frac{a^2 b^2}{L^2} \pi + \frac{ab}{kb}$$

(28) $\left(\frac{u^2}{T^3} + 1\right) \ln\left(\frac{T}{u^2}\right) - \frac{1}{u} \ln\left(\frac{T}{u^2}\right) = x$

$$(22) \quad \left(3 \frac{10.5 \text{ W/s}}{1} + 1 \right) \cdot 2 \frac{1.0}{10.5 \text{ W/s}} - \frac{3}{10.5} = x$$

Using the voltage definition

$$V(x) = \int_0^x \mathcal{E}(x) \frac{dx}{d\mathcal{E}} d\mathcal{E}, \quad (37)$$

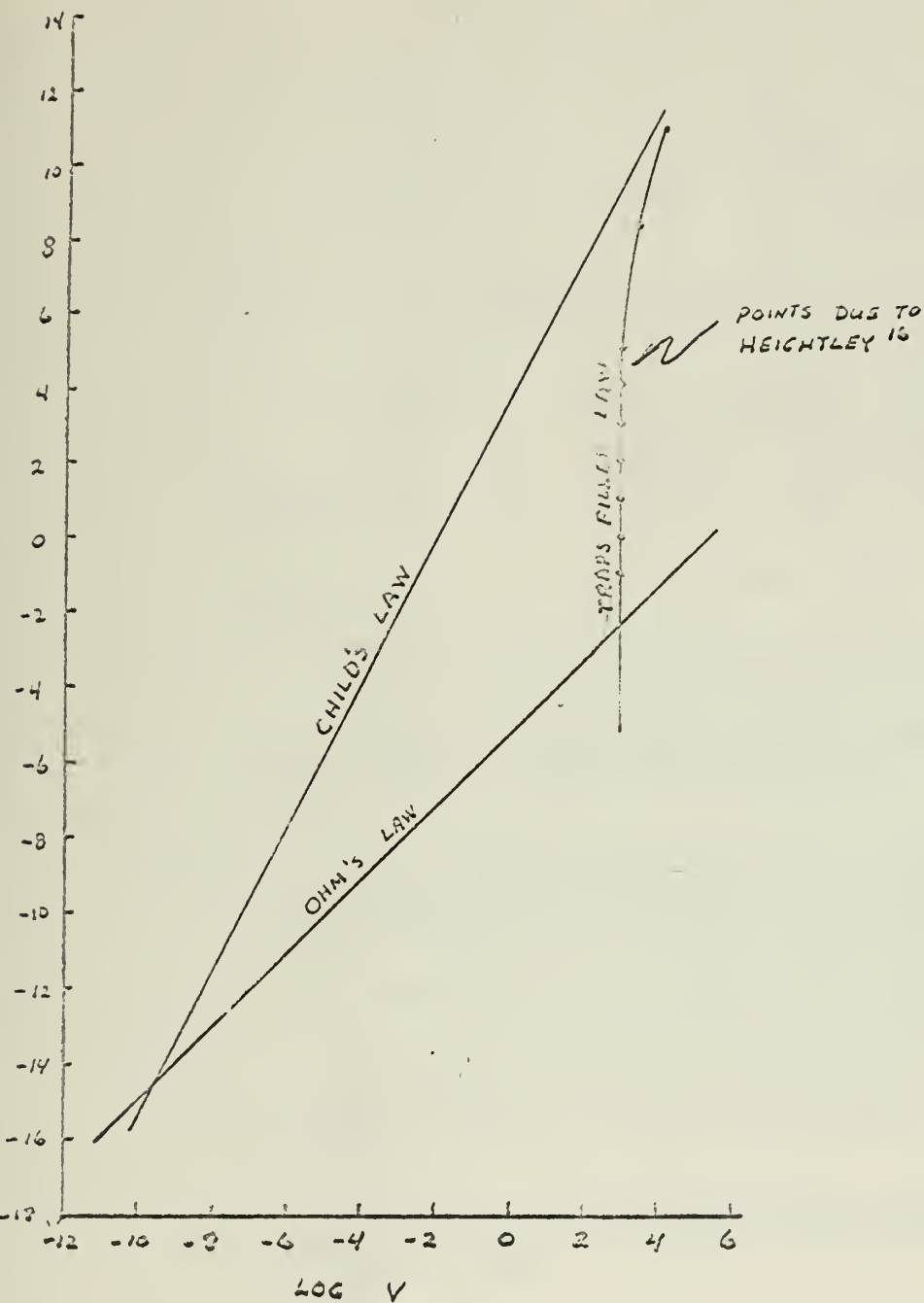
we have

$$V(x) = \frac{\mathcal{E}}{eN_t} \left[\frac{\mathcal{E}^2(x)}{2} - \frac{J}{eN_t\mu} + \frac{J^2}{e^2N_t^2\mu^2} \ln \left(1 + \frac{eN_t\mu}{J} \mathcal{E} \right) \right] \quad (38)$$

(36) and (38) do not form a very tractable set of parametric equations, but a J vs $V(d)$ relation may be obtained by assuming a J in (36) and solving for $\mathcal{E}(d)$. This value of $\mathcal{E}(d)$ is substituted into (38) to obtain $V(d)$. This has been done by Heightley for the case $N_t = 10^{17}/\text{cm}^3$, $\mu = 200 \text{ cm}^2/\text{volt-sec}$, $\epsilon = 11\epsilon_0$, & $\rho \approx 10^{-2} \text{ g/cm}^3$. He obtains the results in figure 10.

In figure 11, we see a triangle formed by Ohm's law, Child's law for solids, and the traps-filled-limit (TFL) law. We state that the J - V curve must lie within this triangle because:²

- (a) J cannot lie below Ohm's law since carriers injected at the cathode can only enhance the current flow.
- (b) J cannot lie above Child's law since this represents the case where all injected carriers add to the current flow.
- (c) J cannot lie below TFL law since this represents the case when the least number of injected carriers contribute to the current.



LIMITING $\log J$ VS $\log V$ CHARACTERISTICS
FOR SPACE-CHARGE-LIMITED CURRENT WITH TRAPS

FIGURE 10

REFERENCES

1. A. Rose, Phys. Rev., 97, 1538 (1955).
2. M. A. Lampert, Phys. Rev., 103, 1649 (1956).
3. G. T. Wright, Proc. I.E.E., 106B, 915 (1959).
4. J. Lindmayer, J. Reynolds, & C. Wrigley, J. Appl. Phys. 34, 809 (1963).
5. For a brief summary of references 1-4, see Appendix of this paper.
6. R. W. Smith & A. Rose, Phys. Rev., 97, 1531 (1955).
7. J. W. Mac Arthur, Electrical Properties of Thin Films of CdS, (Report 7848 - 7849 - R - 4, Servomechanisms Laboratory, MIT, Cambridge, 1958), pp 29-36.
8. J. Dresner & F. V. Shallcross, Solid-State Elect. 5, 205 (1962).
9. R. H. Bube, Phys. Rev. 99, 1105 (1955).
10. M. S. Osman, A Mechanism for 1/f Noise of Thin Evaporated Metal Films, (Report ESL-R-149, MIT, Cambridge, 1962), p 49.
11. K. Weiss, German Patent 837,424. Patent describes process of obtaining specific resistances of $10^8 - 10^{10} \Omega\text{-cm}$ with substrate temperatures from 380°C to 420°C.
12. T. J. Lewis, Phys. Rev. 101, 1694 (1956).
13. S. R. Pollack, J. Appl. Phys. 34, 877 (1963).
14. Lampert has shown that the maximum deviation from the average field is a factor of 2. (See reference 2.)
15. N. F. Mott and R. W. Gurney, Electronic Processes in Ionic Crystals (Oxford University Press, New York, 1940), first edition, p. 172.
16. J. D. Heightley, Private Communication.

Thesis
M12

McAfee

70455

Current flow in a
thin film cadmium
sulfide diode.

MR 10 64

DISPLAY

Thesis
M12

McAfee

70455

Current flow in a
thin film cadmium
sulfide diode.

thesM12

Current flow in a thin film cadmium sulf



3 2768 001 88679 9

DUDLEY KNOX LIBRARY